Unique Haplotypes in *OPN1LW* as a Common Cause of High Myopia With or Without Protanopia: A Potential Window Into Myopic Mechanism

Yingwei Wang,[1] Wenmin Sun,[1] Xueshan Xiao,[1] Yi Jiang,[1] Jiamin Ouyang,[1] Junwen Wang,[1] Zhen Yi,[1] Shiqiang Li,[1] Xiaoyun Jia,[1] Panfeng Wang,[1] J. Fielding Hejtmancik,[2] and Qingjiong Zhang[1,]

[1]State Key Laboratory of Ophthalmology, Zhongshan Ophthalmic Center, Sun Yat-sen University, Guangdong Provincial Key Laboratory of Ophthalmology and Visual Science, Guangzhou, China
[2]Ophthalmic Molecular Genetics Section, Ophthalmic Genetics and Visual Function Branch, National Eye Institute, Rockville, Maryland, United States

Correspondence: Qingjiong Zhang, Pediatric and Genetic Eye Clinic, Zhongshan Ophthalmic Center, Sun Yat-sen University, 54 Xianlie Road, Guangzhou 510060, China; zhangqji@mail.sysu.edu.cn or zhangqingjiong@gzzoc.com.

YW, WS, and XX contributed equally to this work.

Received: January 15, 2023
Accepted: April 6, 2023
Published: April 25, 2023

Citation: Wang Y, Sun W, Xiao X, et al. Unique haplotypes in *OPN1LW* as a common cause of high myopia with or without protanopia: A potential window into myopic mechanism. *Invest Ophthalmol Vis Sci.* 2023;64(4):29. https://doi.org/10.1167/iovs.64.4.29

Purpose. Specific haplotypes (LVAVA, LIVVA, and LIAVA) formed by five polymorphisms (p.L153M, p.V171I, p.A174V, p.I178V, and p.S180A in exon 3 of *OPN1LW*) that cause partial or complete exon skipping have been reported as unique genetic causes of high myopia with or without colorblindness. This study aimed to identify the contribution of *OPN1LW* to early-onset high myopia (eoHM) and the molecular basis underlying eoHM with or without colorblindness.

Methods. Comparative analysis of exome sequencing data was conducted for 1226 families with eoHM and 9304 families with other eye conditions. *OPN1LW* variants detected by targeted or whole exome sequencing were confirmed by long-range amplification and Sanger sequencing, together with segregation analysis. The clinical data were thoroughly analyzed.

Results. Unique haplotypes and truncation variants in *OPN1LW* were detected exclusively in 68 of 1226 families with eoHM but in none of the 9304 families with other visual diseases ($P = 1.63 \times 10^{-63}$). Four classes of variants were identified: haplotypes causing partial splicing defects in *OPN1LW* (LVAVA or LIVVA in 31 families), LVAVA in *OPN1LW-OPN1MW* hybrid gene (in 3 families), LIAVA in *OPN1LW* (in 29 families), and truncations in *OPN1LW* (in 5 families). The first class causes partial loss of red photopigments, whereas the latter three result in complete loss of red photopigments. This is different from the replacement of red with green owing to unequal re-arrangement causing red-green colorblindness alone. Of the 68 families, 42 affected male patients (31 families) with the first class of variants (LVAVA or LIVVA in *OPN1LW*) had eoHM alone, whereas 37 male patients with the latter 3 classes had eoHM with protanopia. Adaptive optics retinal imaging demonstrated reduced cone regularity and density in men with eoHM caused by *OPN1LW* variants compared to those patients with eoHM and without *OPN1LW* variants.

Conclusion. Based on the 68 families with unique variants in *OPN1LW*, our study provides firm evidence that the two different phenotypes (eoHM with or without colorblindness) are caused by two different classes of variants (partial splicing-effect haplotypes or complete splicing-effect haplotypes/truncation variants, respectively). The contribution of *OPN1LW* to eoHM (isolated and syndromic) was characterized by *OPN1LW* variants found in 5.5% (68/1226) of the eoHM families, making it the second most common cause of monogenic eoHM alone (2.4%) and a frequent cause of syndromic monogenic eoHM with colorblindness. Such haplotypes, in which each individual variant alone is considered a benign polymorphism, are potential candidates for other hereditary diseases with causes of missing genetic defects.

Keywords: *OPN1LW*, early-onset high myopia (eoHM), haplotype, colorblindness, cone

Color vision is determined by genes encoding three different cone photopigment types that were sensitive to long (*OPN1LW*), middle (*OPN1MW*), and short (*OPN1SW*) wavelengths.[1,2] *OPN1LW* and *OPN1MW*, located on Xq28 and arranged in a head-to-tail tandem array, share 98% sequence identity.[2,3] It is well known that unequal

homologous recombination between *OPN1LW* and *OPN1MW* is frequently observed as the origin of the molecular defects that cause red-green color vision deficiency, the most common Mendelian trait in humans.[1–4] In addition, the inactivation of the *OPN1LW* and *OPN1MW* resulted in blue cone monochromacy (BCM).[5]

X-linked early-onset high myopia (eoHM) with colorblindness and/or cone dysfunction or other allied abnormalities, also called Bornholm eye disease, has been mapped to Xq28 and has been well-studied clinically and genetically.[6–8] Surprisingly, this syndrome is caused by unique haplotypes formed by a combination of 5 polymorphic missense variants (p.L153M, p.V171I, p.A174V, p.I178V, and p.S180A) in exon 3 of *OPN1LW* (LVAVA and LIAVA).[8–11] Subsequent studies demonstrated that LVAVA leads to the partial skipping of exon 3 (a mosaic truncation effect), whereas LIAVA leads to the complete skipping of exon 3 (similar to truncation variants).[12–14] Similarly, eoHM with colorblindness can be caused by truncation variants in *OPN1LW*.[15] Recently, a novel haplotype LIVVA in *OPN1LW* that causes a partial splicing effect was also found to cause X-linked cone dystrophy with severe myopia.[16] X-linked eoHM alone, without colorblindness or other allied anomalies, was also mapped to Xq28 and was shown to result from the LVAVA haplotype in *OPN1LW* in our previous studies.[15,17] One of our recent studies suggested that LVAVA haplotypes in *OPN1LW* may be the second most common cause of eoHM after *ARR3*.[18]

It is interesting to know the underlying molecular basis through which some haplotypes cause eoHM alone, whereas others cause eoHM with colorblindness (or Bornholm eye disease). Moreover, if there is a difference in terms of genetic defects, what is the proportion of eoHMs with and without colorblindness? In the current study, based on the analysis of targeted and whole exome sequencing data with variants detected in *OPN1LW* in our laboratory, the haplotypes of *OPN1LW* were thoroughly analyzed in probands from 1226 families with syndromic or nonsyndromic eoHM and compared with probands from 9304 families with other eye conditions. Unique variants of *OPN1LW* were confirmed using long-range amplification, Sanger sequencing, and segregation analysis. The clinical data were thoroughly evaluated, particularly refractive status, fundus changes, and color vision. Overall, 4 classes of unique variants were detected in 68 of the 1226 families with eoHM but in none of the 9304 families with other eye conditions. These included haplotypes that cause a partial splicing defect in *OPN1LW* (LVAVA or LIVVA, in 31 families), LVAVA in *L-M* hybrid gene (in 3 families), a complete splicing defect haplotype (LIAVA) in *OPN1LW* (in 29 families), and truncations in *OPN1LW* (in 5 families). Of these, 42 male patients from 31 families with partial splicing-effect haplotypes in *OPN1LW* had eoHM alone, and 37 male patients from the remaining 37 families had eoHM with protanopia. This study, based on a large cohort of Chinese patients with unique variants of *OPN1LW*, further confirmed that different *OPN1LW* haplotypes are associated with eoHM alone and eoHM with colorblindness. Furthermore, our data suggested that unique *OPN1LW* variants are a common cause of both eoHM alone and syndromic eoHM. This identification of unique haplotypes as a common cause of distinct phenotypes in a gene well-known for other diseases reminds us that cis combinations of individually benign polymorphisms should be explored as a potential cause for other hereditary diseases with "missing" genetic defects.

Methods

Subjects

This study was approved by the Institutional Review Board of Zhongshan Ophthalmic Center. A total of 1226 families with eoHM and 9304 unrelated probands with other eye conditions were recruited from the Pediatric and Genetic Clinic of the Zhongshan Ophthalmic Center, Guangzhou, China. Written informed consent was obtained from the participants or their guardians in accordance with the tenets of the Declaration of Helsinki. Peripheral venous blood samples were obtained, and genomic DNA was isolated using previously described methods.[19] The clinical data of each participant were collected, and all participants underwent a comprehensive ocular examination.

Genetic Analysis

Targeted exome sequencing (TES) and whole exome sequencing (WES) were performed on leukocyte genomic DNA samples from all 1226 eoHM probands and 9304 unrelated probands with other ocular disorders, as previously described.[20–22] Based on the exome sequencing data, 5 significant polymorphic variants in exon 3 of *OPN1LW* (p.L153M, p.V171I, p.A174V, p.I178V, and p.S180A) were screened, and their combination formed high-risk haplotypes in *OPN1LW*. Individuals with one of the five high-risk *OPN1LW* haplotypes in hemizygous status that have been reported to cause vision disorders,[16,23] including probands with LIAVA haplotype (p.V171I, p.I178V, and p.S180A but not p.L153M and p.A174V), individuals with LVAVA (p.I178V and p.S180A but not p.L153M, p.V171I, and p.A174V), individuals with LIVVA haplotype (p.V171I, p.A174V, p.I178V, and p.S180A but not p.L153M), probands with the LIAVS haplotype (p.V171I and p.I178V but not p.L153M, p.A174V, and p.S180A), and individuals with MIAVA (p.L153M, p.V171I, p.I178V, and p.S180A but not p.A174V), were selected from the exome sequencing data. In addition, probands detected with truncation variants in *OPN1LW* by TES or WES were chosen. Probands detected with one of the five high-risk haplotypes mentioned above or truncation variants in *OPN1LW* in hemizygous status by TES or WES were further confirmed using a previously reported method that uses long-range polymerase chain reaction (PCR) to specifically amplify the first gene of the opsin gene arrays.[15,24] Long-range PCR was performed using the LA Taq Hot Start protocol (Takara, Kyoto, Japan). The product of the long-range PCR was used as the template in a second PCR reaction to amplify exons 2 to 5, as described previously.[15] Finally, Sanger sequencing was used to determine the sequence of the first gene and any variants (Supplementary Fig. S1).[20]

Clinical Assessment

The clinical data of the affected male patients with the LVAVA haplotype, LIVVA haplotype, LIAVA haplotype, and truncation variants were reviewed in detail, including the age of onset, age at examination, chief complaint, other symptoms, and family history. A comprehensive ocular evaluation was performed, including refractive errors, best-corrected visual acuity (BCVA), color vision function tests (Ishihara plates and Farnsworth-Munsell Dichotomous D-15 Test), axial length, color fundus photography, fundus

Investigative Ophthalmology & Visual Science

autofluorescence (FAF), wild-field scanning laser ophthalmoscopy (SLO; Optos, UK, and ZEISS CLARUS 500, Germany), optical coherence tomography (OCT), and electroretinography (ERG), in accordance with the International Society for Clinical Electrophysiology of Vision standard.

Adaptive Optics Retinal Imaging

The status of the cone photoreceptors located in the foveal and parafoveal areas was obtained and analyzed using an Adaptive Optics (AO) retinal camera (rtx1; Imagine Eyes, Orsay, France). At least 5 retinal imaging scans were acquired, including one foveal area and 4 perifoveal areas (temporally, nasally, superiorly, and inferiorly) of the retina, which was 2 degrees (approximately 540–600 µm) away from the foveal center with a standardized 80 × 80 µm sampling window size. The images captured from each participant were analyzed using the AO detect processing software, including cone density, regularity, dispersion, and spacing.

Statistical Analysis

Statistical analysis was performed using SPSS Statistics 25.0, and P values less than 0.05 were considered statistically significant. The Mann-Whitney U test was performed to compare refractive errors between affected male patients with partial splicing effects (LVAVA and LIVVA) in *OPN1LW* and those with completely splicing effects (LIAVA) or truncation variants in *OPN1LW*. The χ^2 test was conducted to compare the impaired level of cones between the affected male patients with the haplotype having a partial skipping impact and those with variants causing complete loss of L-cone function. The unpaired t test was performed to compare the parameters of cone mosaic status analyzed by AO detect between affected male patients with unique variants in *OPN1LW*, female carriers with variants in *OPN1LW* in heterozygous status, and controls who were matched for age, sex, refraction, and BCVA but did not carry high-risk haplotypes in *OPN1LW*. The correlation between cone density and BCVA in affected male patients was determined using Spearman's correlation analysis.

Results

Identification of Families With Unique Variants in *OPN1LW*

To gain a comprehensive understanding of the genetic and clinical features of *OPN1LW*-associated eoHM, three eoHM families in our previous study were included.[15] Based on the analysis of the TES and WES data of both 1226 eoHM probands and 9304 probands with other ocular conditions, 68 probands were found with high-risk haplotypes or truncation variants in *OPN1LW*, including 26 detected with LVAVA (p.[L153; V171; A174; V178; A180]), 29 detected with LIAVA (p.[L153; I171; A174; V178; A180]), 8 detected with LIVVA (p.[L153; I171; V174; V178; A180]), and 5 probands with truncation variants (details below). Unique variants in *OPN1LW* were found in 68 probands of the 1226 families with eoHM but none of the 9304 families with other eye diseases ($P = 1.63 \times 10^{-63}$). The 68 probands from the 1226 eoHM families were further confirmed by long-range PCR, secondary PCR, and Sanger sequencing of the entire *OPN1LW* gene, which identified 4 classes of unique haplotypes in a structurally intact opsin gene cluster (Fig. 1A). The LVAVA and LIVVA haplotypes in *OPN1LW*, which produce large amounts of aberrantly spliced transcripts while preserving low levels of correctly spliced red photopigment transcripts, were identified in 31 families (23 with LVAVA and 8 with LIVVA; Fig. 1B). The LVAVA in *L-M* hybrid gene (exons 2 and 3 belonging to *OPN1LW* and exons 4 and 5 belonging to *OPN1MW*), which encodes photopigments with a peak spectral sensitivity of green and produces a low level of functional photopigments because of the incomplete splicing impact of LVAVA, was identified in three families (Fig. 1C). The LIAVA haplotype of *OPN1LW*, in which exon 3 was aberrantly spliced and produced no functional red photopigments, was detected in 29 families (Fig. 1D). The truncation variants of *OPN1LW* were confirmed in five families (Fig. 1E). None of the five truncation variants, including one previously reported variant (c.617_620dup/p.F208Rfs*51) or four novel variants (c.427_433dup/p.A145Vfs*23, c.518_519insC/p.A174Cfs*84, c.739C>T/p.R247*, and c.757C>T/p.Q253*) were present in the gnomAD database. These unique variants in *OPN1LW* were verified by Sanger sequencing and confirmed by cosegregation in 45 families (15 with LVAVA in *OPN1LW*, 5 with LIVVA in *OPN1LW*, 20 with LIAVA in *OPN1LW*, 3 with LVAVA in *L-M* hybrid, and 2 with truncations; Fig. 2, Supplementary Figs. S2–S6). Classical X-linked recessive inheritance was observed in 47 families. No hemizygous individuals with MIAVA or LIAVS haplotypes were identified.

Clinical Characterization

All 79 male patients carrying hemizygous variants in *OPN1LW* from the 68 families were diagnosed with eoHM, including 42 male patients from 31 families with partial splicing-effect haplotypes in *OPN1LW* who had eoHM alone and 37 male patients with the latter three types who had eoHM and protanopia. All 79 male patients complained of blurred vision since early childhood; however, none showed nystagmus, severe photophobia, or night blindness. Among the 77 affected male patients with refraction data, 89.6% (69/77) had a refractive error of ≤−5.00 diopters (D; or axial length ≥25 mm) before 7 years of age, whereas the remaining 6.5% (5/77) who were older than 18 years at their first visit to our clinic had refractive errors ≤−10.00 D. The available equivalent spherical data of all affected males ranged from −3.75 D to −22.00 D (median = –9.38 D, interquartile range [IQR] = approximately −7.13 D to −11.09 D; Supplementary Fig. S7A), in whom three male patients had moderate myopia in early visit but develop myopia to −5.00 D or greater in follow-up visit by age of 7 years. For example, follow-up refraction recordings were accessible for 20 affected male patients, showing a gradually increased trend with age up to 15 years of age (see Supplementary Fig. S7B). Two (8928-IV4 and 18972-II2) had equivalent spherical refractions of approximately −4.00 D at first presentation when they were less than 4 years old, but with progression reached −6.00 D by the age of 6 years. There were no differences in equivalent spherical diopters between male patients with partial splicing-effect haplotypes in *OPN1LW* (LVAVA and LIVVA) and those with loss of function variants in *OPN1LW* (LIAVA and truncations; see Supplementary Fig. S7D). The astigmatism diopter values were available from 75 of the 77 affected male patients, ranged from −0.25 D to −5.00 D (median = −2.00 D, IQR = approximately −1.25 D

Investigative Ophthalmology & Visual Science

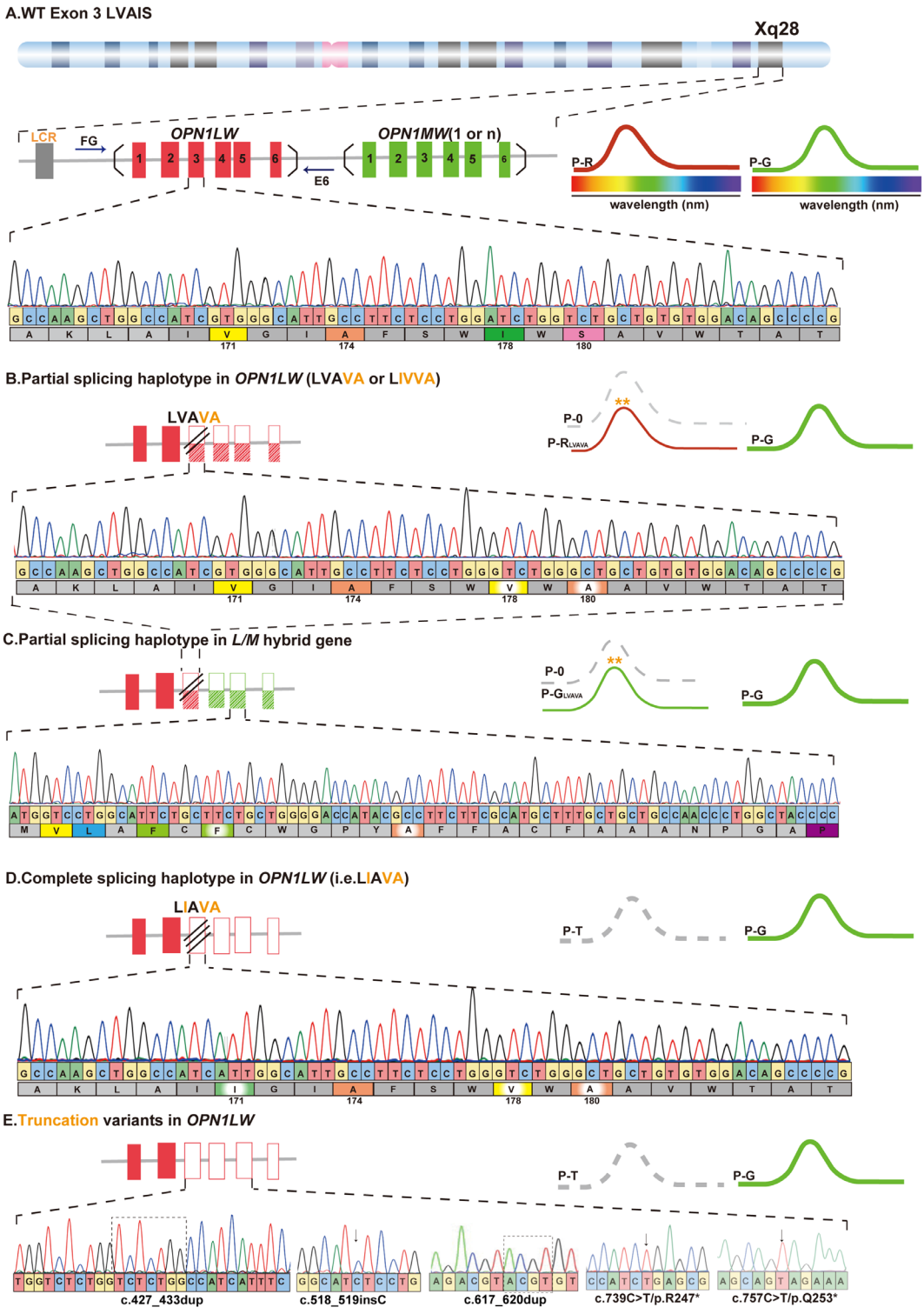

Figure 1. Structure of the four classes of unique variants in *OPN1LW* identified in our study. (**A**) Wild-type *OPN1LW* and *OPN1MW* are arranged in a head-to-tail tandem array on chromosome Xq28, encoding red and green cone photopigments maximally sensitive to long and middle wavelengths, respectively. Intact opsin arrays consisting of one *OPN1LW* with single nucleotide polymorphisms (p. [L153; V171; A174; I178; S180]) in exon 3 and one or more *OPN1MW* genes with only the first normally expressed are responsible for normal trichromatic vision. (**B**) LVAVA (p. [L153; V171; A174; V178; A180]) and LIVVA (p. [L153; I171; V174; V178; A180]) with a partial splicing defect in *OPN1LW* causing functional loss of most *L*-cone red photopigment and a few reserved transcripts encoding functional red opsin (mosaics status). (**C**) LVAVA in *L-M* hybrid gene (exons 2 and 3 belonging to *OPN1LW* while exons 4 and 5 belonging to *OPN1MW*) with amino acids in exon 5 of *OPN1MW*, which are important for most spectral sensitivity, leads to no functional red photopigment and partially damaged *M* cones due to the LVAVA haplotype. (**D**) LIAVA (p. [L153; I171; A174; V178; A180]) with complete splicing in *OPN1LW* causes no functional *L*-cones. (**E**) Truncation mutations in exon 3, exon 4, and exon 5 of *OPN1LW* results in the identical lack of red signaling as the LIAVA haplotype, causing the complete aberrant splicing and premature termination. The FG and E6 were primers for amplifying the first gene of the opsin array.

Investigative Ophthalmology & Visual Science

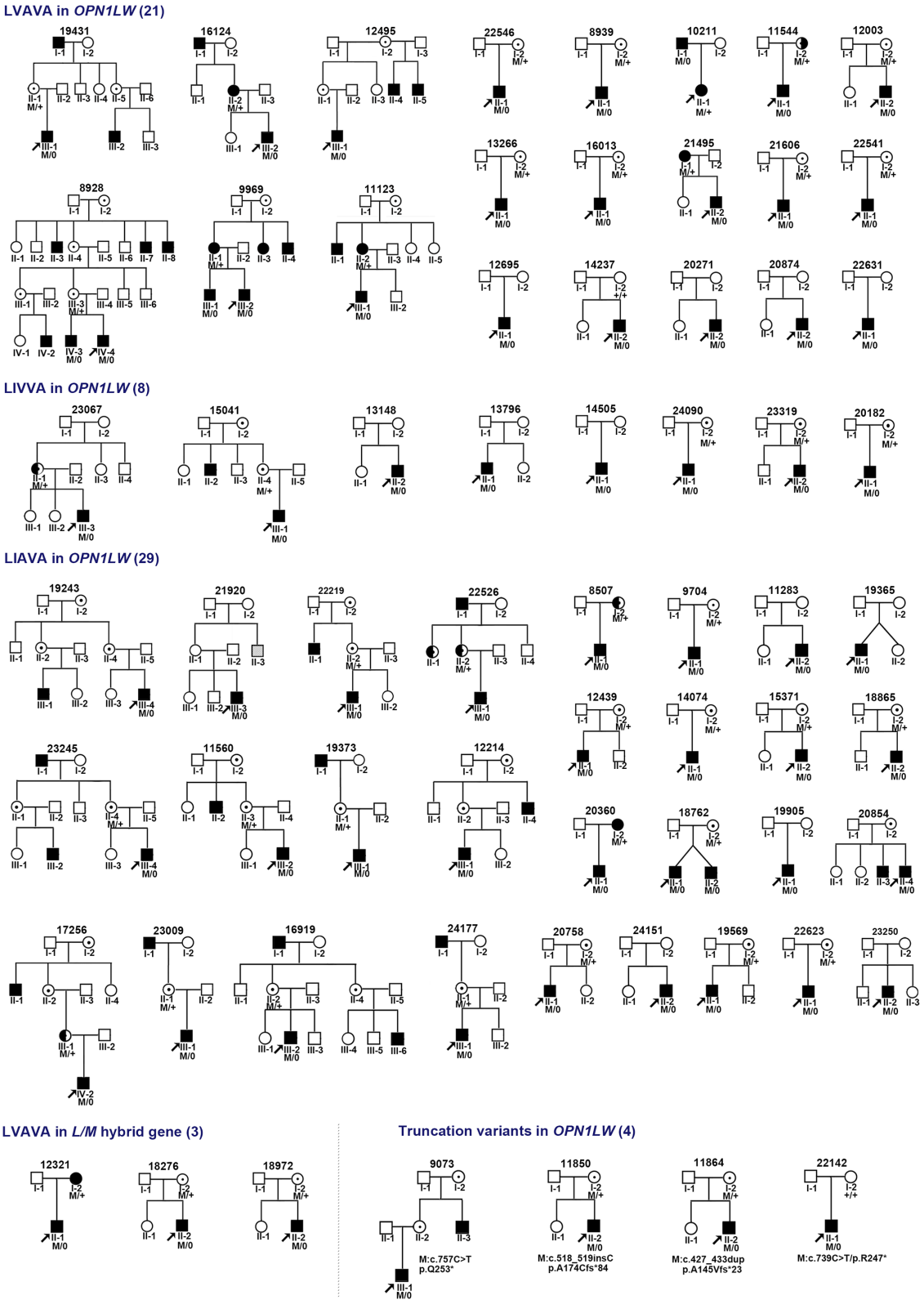

Figure 2. Pedigrees of 65 newly identified families with unique variants in *OPN1LW*. Twenty-one families were identified with the LVAVA haplotype in *OPN1LW*, 8 families were identified with the LIVVA haplotype in *OPN1LW*, 29 families were identified with the LIAVA haplotype in *OPN1LW*, 3 families had the LVAVA haplotype in *L-M* hybrid gene, and 4 families had truncation variants in *OPN1LW*. The *squares* represent male individuals, and the *circles* represent female individuals. The *filled squares* and *circles* indicate affected male and affected female patients, respectively. Heterozygous female carriers are indicated by a *circle with a dot in the center*. A *half-filled circle* indicates a female carrier with high myopia in one eye. Probands in each family are indicated by *arrows*. The family numbers are located above the pedigrees.

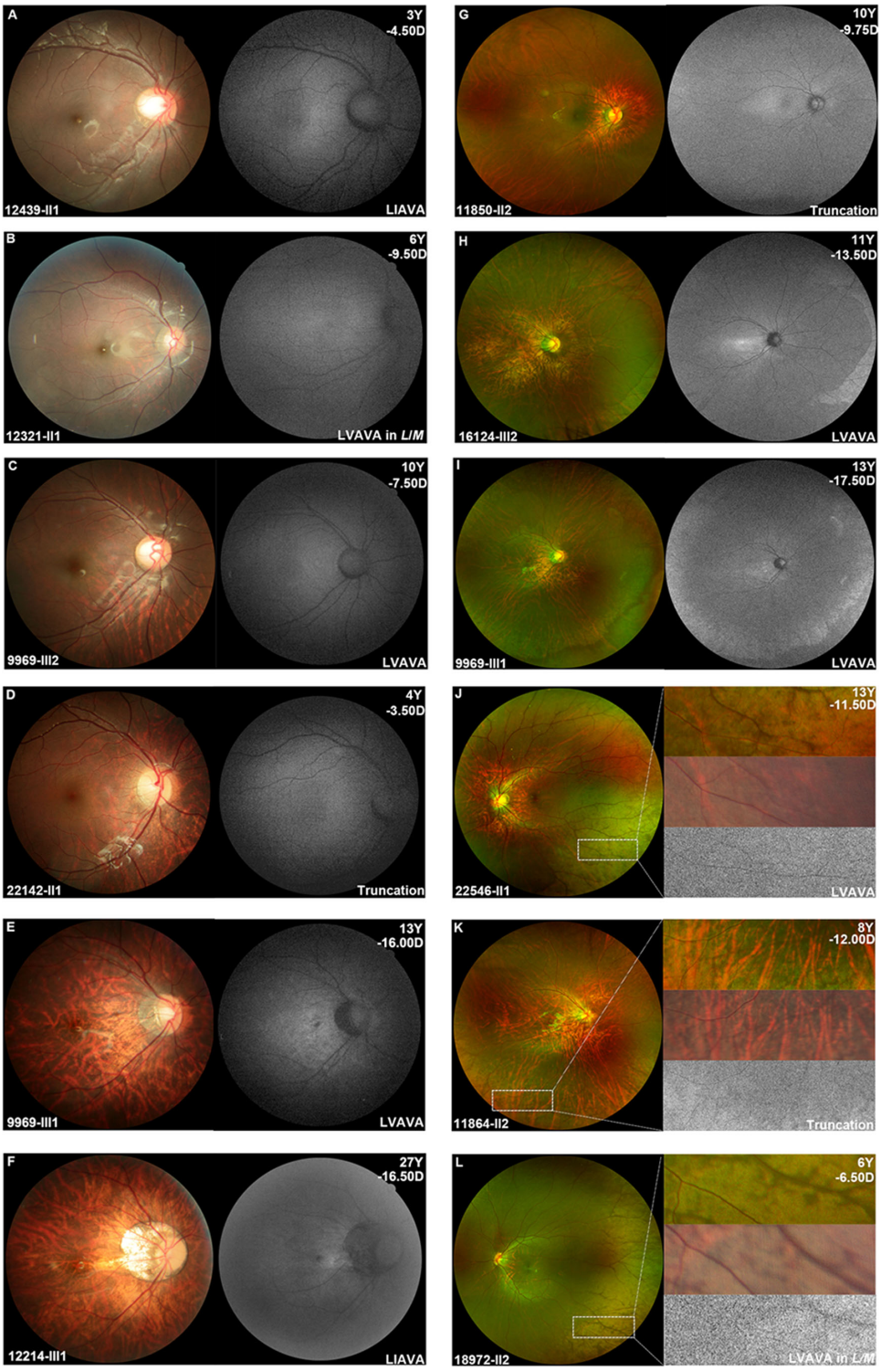

Figure 3. Posterior color fundus photography, autofluorescence images, and wide-field fundus examinations of patients with unique variant types of *OPN1LW* as indicated in the plates. (**A, B**) A few patients showed a relatively normal-appearing fundus (C0). (**C, D**) Most patients presented with tessellated changes in the posterior retina and normal-appearing autofluorescence (C1). (**E, F**) Some patients had slightly yellowish-white chorioretinal atrophy, especially around the optic nerve (C2). Hyper-autofluorescent changes in the macular region were observed in some patients with C2 myopic fundus changes. (**G**) Two-thirds of the patients with a wide-field fundus examination showed tessellated fundus changes with corresponding normal autofluorescence. (**H, I**) The remaining patients presented with borderline pigmentary changes in the peripheral retina, observed as hyper-hypo autofluorescence changes on wild-field fundus autofluorescence images. (**J-L** A few patients showed obvious peripheral pigmentary degeneration on wild-field scanning laser ophthalmoscopy, which was not observed (**J** and **K**) or appeared relatively milder (**L**) on color fundus photography and showed normal autofluorescence. The right parts of the **J** to **L** images correspond to magnified images of the peripheral retinal area, in which the upper is captured by wild-field scanning laser ophthalmoscopy, the middle shows an enlarged color fundus, and the lower shows fundus autofluorescence.

Investigative Ophthalmology & Visual Science

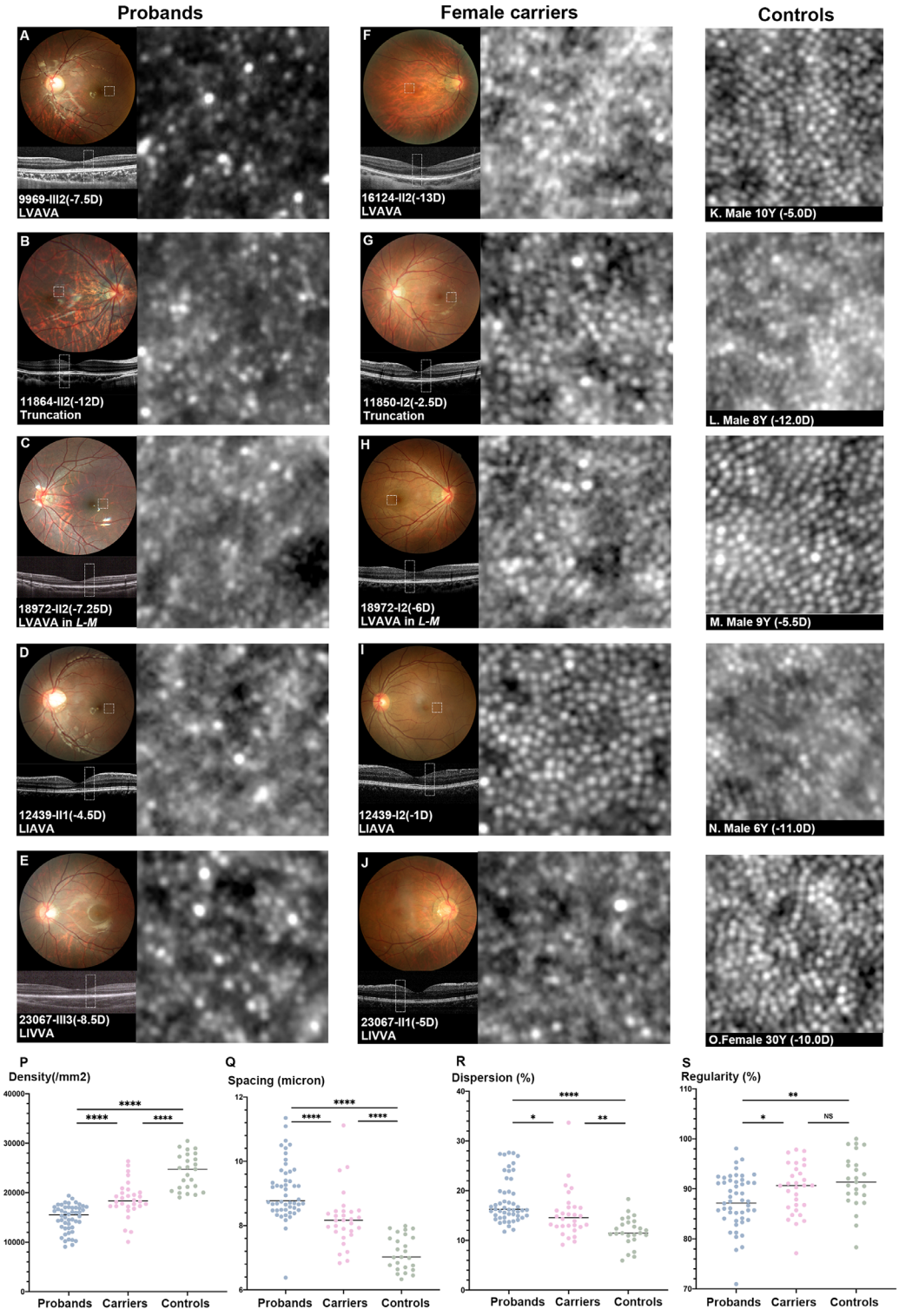

Figure 4. Adaptive optics (AO) retinal imaging of affected male patients with different types of unique variants in *OPN1LW*, heterozygous female carriers, and control individuals matched for sex, age, refraction, and BCVA to affected male patients or female carriers. All AO retinal imaging captured the cone cells at the 2 degrees temporal position of the central fovea. (**A-D**) Affected male patients with four classes of unique variants in *OPN1LW* presented with variable disruption of cone mosaic status. (**E-H**) Female carriers with different types of unique *OPN1LW* variants in heterozygous status presented with a relatively less disruptive cone mosaic state than affected male patients. (**I-L**) Control individuals matched for sex, age, refraction, and BCVA to affected male patients or female carriers with high myopia but without high-risk haplotypes or truncation variants in *OPN1LW* showed a relatively larger cone density. (**M-P**) Scatter diagrams comparing the regularity, density, dispersion, and spacing of cones between the affected probands, female carriers, and control individuals. The affected male patients showed decreased regularity and density but increased dispersion and spacing of cones compared with carriers and controls. The *asterisks* represent statistically significant differences: *, P < 0.05; **, *P* < 0.01; ***, *P* < 0.001, ****, *P* < 0.0001.

Investigative Ophthalmology & Visual Science

to −3.00 D), and 60 of them (80.0%) had astigmatism ≤−1.00 D. BCVA was available for 55 affected male patients and ranged from 0.04 (in one patient with retinal detachment) to 1.0 (median = 0.5, IQR = 0.4–0.7), with 85.5% (47/55) obtaining a BCVA no less than 0.3 (see Supplementary Fig. S6C). The remaining 8 male patients with BCVA less than 0.3 included 5 children younger than 4 years of age and 3 individuals over 35 years old. Color vision testing was conducted on 57 affected male patients, of whom 31 with a partial splicing-effect haplotype in *OPN1LW* had normal color vision (26 with LVAVA and 5 with LIVVA), and the remaining 25 affected male patients (18 with LIAVA in *OPN1LW*, 3 with LVAVA in a hybrid gene, and 4 with truncation variants) had protanopia.

All 73 affected male patients with available posterior color fundus photographs presented with high myopia changes and were assessed according to the META-PM classification.[25] A relatively normal posterior retina without significant myopic changes (C0) was observed in 6.8% (5/73) of the male patients (Figs. 3A, 3B). Tessellated changes were concentrated in the posterior retina and more severely around the optic nerve, with visible choroidal vessels (C1) observed in 52.1% (38/73) of the male patients (Figs. 3C, 3D). Yellow-white diffuse chorioretinal atrophy, mainly in the area between the optic nerve and the macula (C2), was found in 34.2% (25/73) of the affected male patients (Figs. 3E, 3F). Well-defined white atrophic patches around the optic nerve (C3) were observed in 6.8% (5/73) of patients. Among the 20 male patients with FAF, 70.0% (14/20) had normal autofluorescence (Fig. 3G) and 30.0% (6/20) showed relatively hyper-autofluorescent changes in the macular region (Figs. 3H, 3I). Thirty-four male patients underwent wide-field fundus examinations, of whom 76.5% (26/34) presented with pigmentation changes at the boundary or a pigmentary disorder in the periphery (Figs. 3H, 3I), 5.9% (2/34) showed lattice-like degeneration, and the remaining 17.6% (6/34) had a normal-appearing peripheral retina. Different degrees of peripheral pigmentary degeneration may manifest differently when viewed using different imaging techniques. Some affected male patients, although showing peripheral pigmentary disturbances in SLO, appeared on color fundus images to have tessellated changes with no pigmentary changes and showed relatively normal autofluorescence on FAF (Figs. 3J-L, Supplementary Fig. S8).

Among the 41 affected males with OCT results, 70.7% (29/41) had normal macular foveal structures, six male patients (five with LIAVA and one with LIVVA) (14.6%) showed thinner outer nuclear layers and disrupted ellipsoid zones, and six male patients older than ten years (14.6%) presented with pathologic myopic macular degeneration (Supplementary Fig. S9). There were no statistically significant differences in the fundus changes or OCT structures between the males with eoHM alone due to the partial splicing-effect haplotypes in *OPN1LW* and those with the latter three types of variants leading to eoHM and protanopia. ERG examinations were available for 11 male patients with the LVAVA haplotype, including 9 with LVAVA in *OPN1LW* and 2 with LVAVA in the *L-M* hybrid gene, 5 of whom had mild cone involvement and normal rod responses, 5 had moderately reduced cone responses and normal or mildly reduced rod responses, and a 40-year-old man had severely reduced cone responses and moderate rod involvement. Two affected male patients with LIVVA presented with severe cone involvement and mildly reduced or normal rod responses. Eighteen male patients with LIAVA or truncation variants underwent ERG examinations, of which moderate cone impairment with normal rod responses was observed in 3 patients, and severely reduced cone responses with various degrees of reduced rod responses were found in 15 male patients (8 with normal or mildly reduced rod responses, 3 with moderate rod involvement, and 4 with severe rod impairment). Statistically significant differences were found in the level of cone impairment between male patients with partial splicing-effect haplotypes and those with loss of function variants (χ^2 test, $P = 0.008$). A total of 53 obligate female carriers were confirmed as heterozygous carriers, of whom 17 had high myopia at an early age (6 had high myopia in one eye only), with 32.1% (17/53) penetrance.

Assessment of Cone Mosaic Status

The mean values of the cone features were calculated and compared for cases (10 affected male patients and 6 female carriers carrying different types of variants in *OPN1LW*) and controls (4 male patients and 1 female patient) matched for age, refraction, and BCVA. Statistically significant differences were identified between the affected male patients and controls in terms of cone regularity (87.1 ± 5.9 vs. 91.5 ± 5.0, $P = 0.003$), density (14886.8 ± 2678.2 vs. 24203.2 ± 3612.1, $P < 0.0001$), dispersion (18.1 ± 4.6 vs. 9.1 ± 0.9, $P < 0.0001$), and spacing (9.1 ± 0.9 vs. 7.2 ± 0.5, $P < 0.0001$). Statistically significant differences were also found between affected male patients and female carriers, who had regularity = 89.9 ± 5.0 ($P = 0.03$), density = 18644.2 ± 3612.1 ($P < 0.0001$), dispersion = 15.3 ± 4.8 ($P = 0.01$), and spacing = 8.2 ± 0.9 ($P < 0.0001$), as well as between female carriers and control individuals ($P < 0.0001$ for density and spacing; $P = 0.002$ for dispersion; Fig. 4). Additionally, no correlation was found between cone density and BCVA of the affected males (Spearman's correlation = 0.233, $P = 0.578$), reflecting the relatively narrow range of variation in which almost all had densities greater than those required for visual acuity greater than 0.3.

Discussion

In this study, unique variants in *OPN1LW* were detected exclusively in 68 of the 1226 families with eoHM but not in other ocular diseases, which was further confirmed by co-segregation analysis. High myopia is a constant phenotype in all affected male patients with unique haplotypes and truncation variants in *OPN1LW*, and the presence of color-blindness is determined by the amount of residual functional red photopigments in the *L*-cones. Unlike partial splicing-effect haplotypes in *OPN1LW* that result in mosaics status with different types of *L*-cones due to partial exon skipping effects, LIAVA haplotype and truncation variants in *OPN1LW* cause complete loss of functional red pigmentations in all *L*-cones though the 5′-prime regions are preserved, and the *L-M* hybrid gene encoding photopigments with the spectral sensitivity of green are impacted by the LVAVA haplotype. Based on the largest Chinese cohort of unique variants of *OPN1LW* to date, our study provides firm evidence that the two different phenotypes are caused by two different classes of variants: eoHM alone with partially truncated *OPN1LW* is due to partial splicing-effect haplotypes (LVAVA

or LIVVA), whereas eoHM with colorblindness results from completely truncated *OPN1LW* due to the complete splicing-effect haplotype (LIAVA) or nonsense/frameshift variants. The partial splicing-effect haplotype (LVAVA) in the *L-M* hybrid gene lead to eoHM with colorblindness due to changes in spectral sensitivity. In combination with our previous analysis, *OPN1LW* was found not only to be the top two most frequently implicated genes for nonsyndromic monogenic eoHM (2.4%), second only to *ARR3* (3.1%),[18] but might be among the top five common causative genes for syndromic monogenic eoHM when patients with colorblindness were included. This is the first time that such unique haplotypes in a well-known gene have been implicated as one of the most common causes of nonsyndromic eoHM. The cone mosaic status observed by AO retinal examination in this study was consistent with that of previous studies.[10,26,27]

Rearrangement of *OPN1LW* and *OPN1MW* has long been well-known to cause red-green color vision deficiency, a common monogenetic disease. Initially, protanopia was reported to be attributed to a single *L-M* hybrid gene or replacement of *OPN1LW* by *OPN1MW*, which results in a single or both opsin genes with green spectrum sensitivity.[4,28] Subsequently, a single *L-M* hybrid gene with an inactivating missense mutation (p.C203R) or truncation variant was shown to result in BCM, a severe phenotype caused by the complete absence of *L* and *M* cone function.[29–31] High homology between *OPN1LW* and *OPNMW* contributes to numerous polymorphisms with allele frequencies greater than 1% in general population.[1] Combination of 5 polymorphisms in exon 3 forms various haplotypes with exon skipping impacts to different degrees. In particular, LVAVA and LIAVA have been reported to be associated with X-linked high myopia with accompanying colorblindness.[8] The LVAVA haplotype was first identified as the cause of nonsyndromic eoHM in our previous studies.[15] Variations in *OPN1LW* showed extensive phenotypic heterogeneity, ranging from severe BCM through isolated color vision deficiency to eoHM with and without colorblindness. Moreover, the important role of *OPN1LW* in high myopia has been underestimated in the past. This study showed a high frequency of *OPN1LW* variants in high myopia, and the mechanism of colorblindness accompanying *OPN1LW*-associated eoHM was clearly elucidated. Although the LVAVA haplotype in the *L-M* hybrid gene and LIAVA and truncation variants in *OPN1LW* presented with intact 5′-prime regions, no functional red photopigments were produced. This is different from color vision deficiency due to the rearrangement of structurally intact opsin gene arrays that occurs through the replacement of red photopigments by green ones without loss of functional photopigments. Whether *OPN1LW*-associated eoHM is accompanied by colorblindness depends on the levels and spectral characteristics of correctly spliced opsin mRNA in the opsin gene arrays caused by the diverse haplotypes of *OPN1LW*.[12–14] In addition to variants in *OPN1LW* causing eoHM, high-risk haplotypes in the highly homologous *OPN1MW* gene have also been reported to be responsible for high myopia through the same mechanism as *OPN1LW* variants. The focus of this study on *OPN1LW*-associated eoHM may have underestimated the contribution of variants in *OPN1LW/OPN1MW* to high myopia, which may increase with the inclusion of families with haplotypes in *OPN1MW* and other potential high-risk haplotypes in the opsin array.

Although our study focused on the genotype profiles and clinical characteristics of *OPN1LW* in male patients, it was also found that 17 of the 53 female carriers of heterozygous *OPN1LW* variants had eoHM, whereas the remaining female carriers were asymptomatic. Because *OPN1LW*-associated eoHM is inherited as a classic X-linked recessive trait, the manifestation of eoHM in a small number of female carriers might be achieved by variations in random X-inactivation, which is also thought to be responsible for some female carriers of other X-linked recessive retinal diseases (e.g. retinal degeneration due to *RPGR*) that show variable phenotypic severity. Perhaps more directly related, this has also been reported in one heterozygous female with BCM.[32–34] Significant asymmetric phenotypes between eyes have also been found in heterozygous female carriers of *RPGR* variants,[35] which may share the same mechanism as six female carriers who presented with eoHM in only one eye. As described in the study by Neitz et al.,[23] based on AO retinal imaging examination, the mechanism by which some female carriers exhibit eoHM might be similar to the cone mosaic mechanism by which affected male patients with the *OPN1LW* variant develop eoHM, that is, mosaic cones with different amounts of photopigments mimicking defocus signals to bipolar cells and related neuronal networks influence the onset of high myopia. Further research on female carriers with unique high-risk haplotypes in *OPN1LW* is expected in the future.

Signals from cones are relayed to bipolar cells, then to ganglion cells that finally transmit impulses to the central nervous system, building an intricate "microcircuit" in the retina. The wiring of this circuitry is private in the central fovea, an *L* or *M* cone privately directs input to an ON and OFF midget circuit, which allows high acuity.[36–38] Opposed signals from *OPN1LW* and *OPN1MW* antagonistically interact with each other and thus form the red-green opponent pathways underlying color vision.[39–41] A widely accepted receptive field in the central retina consists of segregated signals from different cones, including an excitatory central signal from an isolated *L* or *M* cone and inhibitory surrounding signals of nonselective input from different cones through horizontal cells.[36,42–45] High-spatial frequency luminance stimuli from the center opposed with the low-spatial frequency brightness stimuli from the neighbor wirings in the foveal private line midget circuit form the contrast signals which have been found to appear in the early fetal period[46] and to impact the growth process of the eyeball.[26,47–49] Individuals with intact opsin arrays have normal trichromatic vision and emmetropization processes (Fig. 5A, Supplementary Fig. S10A). When the original *L*-cones were replaced by cones with photopigments whose maximum spectral sensitivity was green, the spatial contrast in the visual process was unaffected, although protanopia occurred (Fig. 5B, Supplementary Fig. S10B). A partial splicing-effect haplotype in *OPN1LW* resulted in the various opsin properties in the adjacent cones of a single neighborhood, causing abnormal contrast and stimulating eyeball elongation (Fig. 5C, Supplementary Fig. S10C). When an aberrant mosaic status due to the LVAVA haplotype occurs in *L-M* hybrid gene,[50] both eoHM and protanopia occur (Fig. 5D, Supplementary Fig. S10D). LIAVA and truncations in *OPN1LW* resulted in the complete absence of functional cones with red photopigments, which severely damaged the spatial contrast and led to the loss of the ability to sense red light (Fig. 5E, Supplementary Figs. S10E, S10F). This contrast theory is thought to be the potential causal mechanism not

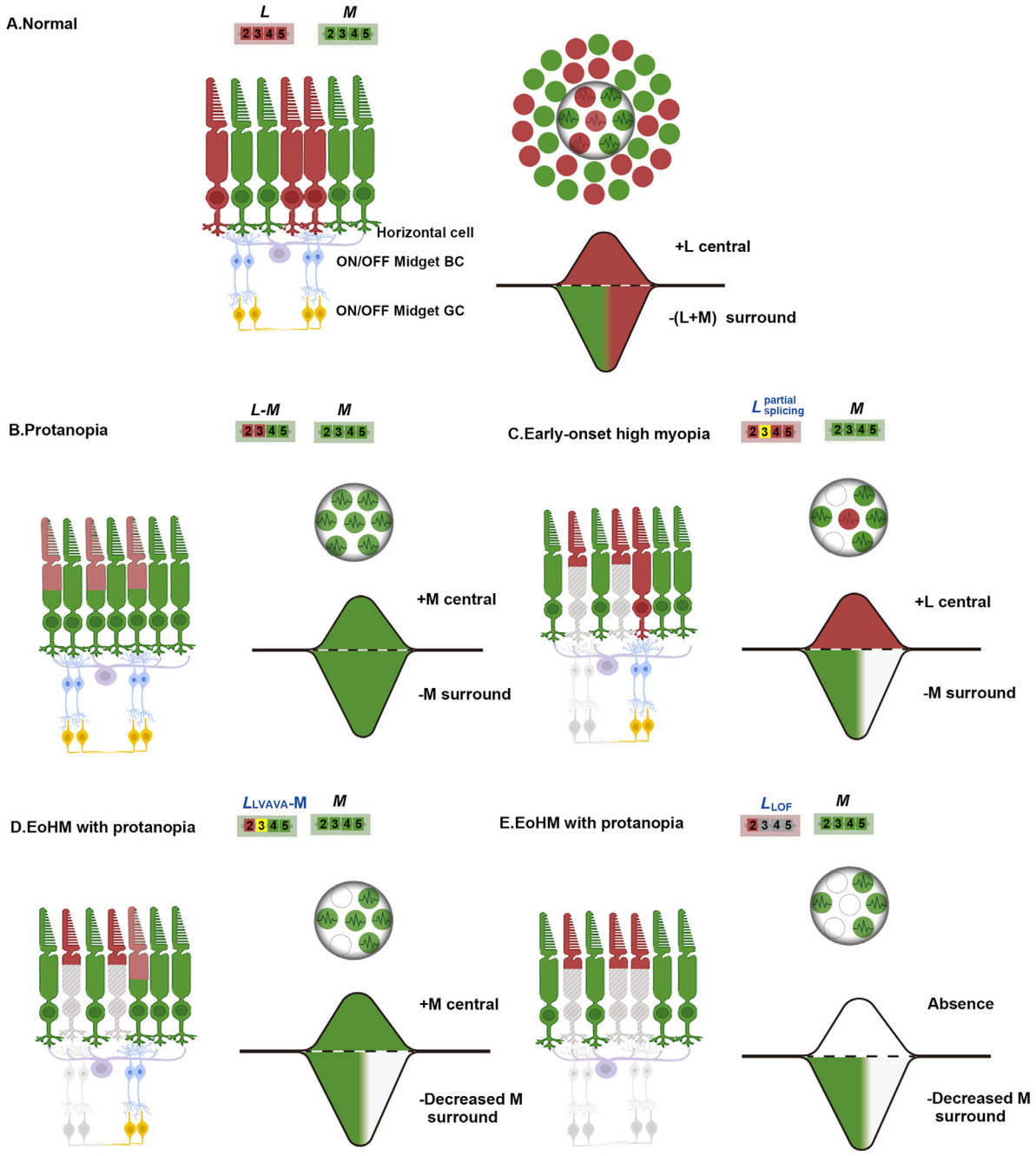

Figure 5. The mixed surround models for red-green spectral opponent explain the potential pathogenesis of eoHM resulting from the four classes of variants in *OPN1LW*. (**A**) In the central retinal area of humans, each cone has a "private line" circuit pathway; that is, each *L* or *M* cone relays signals to an ON midget bipolar cell and an OFF midget bipolar cell, then the bipolar cells further deliver the signal to midget ganglion cells, which form the excitatory center of the receptive field. The H1 horizontal cells non-selectively receive signals from the *L* and *M* cones in the central cone neighbor and form the inhibitory surrounded signal of each receptive field. Using the *L*-cone as the center, for example, signals conducted by this *L*-cone serve as the center signal, and the signals received by the surrounding *L* and *M* cones as opposed signals. The central and surrounded signals form the contrast that affects eye growth. (**B**) The midget circuit diagram for individuals with protanopia due to the presence of *L-M* hybrid gene. Although the *L*-cones are replaced with cones that are maximally sensitive to middle-wavelength light, the generation of excitatory and inhibitory signals are not disrupted. (**C**) In the presence of the partial splicing-effect haplotype in *OPN1LW*, most *L*-cones lose their functional pigmentation, and only a few normally expressed *L*-cones are retained. When the normally expressed *L*-cones act as the central signal in the receptive field, the surrounding inhibitory signal is affected by the absence of functional *L*-cones in the vicinity. The abnormal contrast signal between the central and surround of the receptive field produces blurred vision simulating a refractory error and stimulates the elongation of the eyeball. (**D**) The result of the LVAVA haplotype in hybrid *L-M* gene can be considered a combination of the consequences of a spectrally sensitive change due to the *L-M* hybrid gene and an abnormal spatial contrast signal caused by the LVAVA haplotype in *L-M* gene. (**E**) The LIAVA haplotype and truncation variants in *OPN1LW* lead to the complete loss of functional *L*-cone photopigment. When a nonfunctional *L*-cone acts as the central signal in the receptive field, the surrounding inhibitory signal is also affected by the absence of functional *L*-cones in the neighborhood, which results in early-onset high myopia with protanopia. LOF, loss of function.

Investigative Ophthalmology & Visual Science

only for *OPN1LW*-associated eoHM but also for common juvenile-onset myopia, which has been supported by clinical trials.[47,51] The same mechanisms are thought to underlie the development of high myopia in *ARR3*-associated MYP26 with X-linked female limited inheritance. Thus, the expression of both *ARR3* and *OPN1LW* was cone-specific. Decreased levels of arrestin encoded by *ARR3*, functioning as the desensitizer of opsins, result in increased activity of *L* and *M* cones and enhanced sensitivity of color vision signals, which has been proposed to explain the onset of high myopia secondary to heterozygous variants in *ARR3*.[52] It was hypothesized that the mosaic cone status with adjacent cones expressing different functional opsins of affected female patients with heterozygous variants in *ARR3* is similar to that of affected male patients with hemizygous LVAVA in *OPN1LW* with a partial effect on splicing. The relationship between *OPN1LW* and *ARR3* was similar to that between *RHO* and *SAG*, in which *RHO*, which encodes rhodopsin, was activated when retinal was isomerized from the 11-cis to the all-trans configuration, and its inactivation could be prevented by binding to the arrestin encoded by *SAG*.[53]

In conclusion, variants in *OPN1LW* are a common cause of Mendelian eoHM with or without colorblindness, second only to *ARR3* mutations in isolated eoHM. The proposed mechanism of *OPN1LW*-associated eoHM with or without colorblindness is that variants cause different amounts of functional photopigments, which result in mosaic and disproportional *L*-cones, causing abnormal spatial contrast signals to connect bipolar cells and more distal parts of the associated neuronal network. Proposing a similar mechanism for the top two most frequently implicated genes for eoHM, *ARR3*, and *OPN1LW,* emphasizes the potential significance of *L-M* cones in the myopic mechanism, which may also function in common juvenile-onset myopia. Further studies on cone-bipolar and surrounding neuronal connections in humans or nonhuman primates, may provide a valuable starting point for delineating myopic molecular mechanisms. Additionally, combinations of individually benign variants in the same gene, such as haplotypes in *OPN1LW* and beyond, may underlie a wide variety of diseases, warranting attention to inherited diseases that lack apparent genetic mechanisms.

Acknowledgments

Funded by the National Natural Science Foundation of China (81770965, 81600768), the Science and Technology Planning Projects of Guangzhou (202102010271), and the Fundamental Research Funds of the State Key Laboratory of Ophthalmology. The sponsor or funding organization had no role in the design or conduct of this research.

Contributors: X.X., S.L., X.J., W.S., and Q.Z. recruited the individuals diagnosed with different forms of ocular conditions and collected the clinical records. S.L., X.X., and X.J. prepared the genomic DNA from venous blood. X.X., S.L., P.W., and Q.Z. performed whole exome analysis and targeted exome sequencing. Y.W., Y.J., J.O., J.W., Z.Y., P.W., and Q.Z. participated in the bioinformatics analysis of exome sequencing data and in review and classification of clinical data. Y.W. performed Long-range PCR and Sanger sequence. Q.Z. designed the study. Y.W. and W.S. wrote the manuscript. J.F.F.H. and Q.Z. critically revised the manuscript. All authors reviewed and approved the manuscript. Y.W., W.S., and X.X. contributed equally to this work.

Disclosure: **Y. Wang**, None; **W. Sun**, None; **X. Xiao**, None; **Y. Jiang**, None; **J. Ouyang**, None; **J. Wang**, None; **Z. Yi**, None; **S. Li**, None; **X. Jia**, None; **P. Wang**, None; **J.F. Hejtmancik**, None; **Q. Zhang**, None

References

1. Nathans J, Piantanida TP, Eddy RL, Shows TB, Hogness DS. Molecular genetics of inherited variation in human color vision. *Science*. 1986;232(4747):203–210.
2. Nathans J, Thomas D, Hogness DS. Molecular genetics of human color vision: The genes encoding blue, green, and red pigments. *Science*. 1986;232(4747):193–202.
3. Winderickx J, Battisti L, Hibiya Y, Motulsky AG, Deeb SS. Haplotype diversity in the human red and green opsin genes: Evidence for frequent sequence exchange in exon 3. *Hum Mol Genet*. 1993;2(9):1413–1421.
4. Neitz J, Neitz M. The genetics of normal and defective color vision. *Vision Res*. 2011;51(7):633–651.
5. Ladekjaer-Mikkelsen AS, Rosenberg T, Jørgensen AL. A new mechanism in blue cone monochromatism. *Hum Genet*. 1996;98(4):403–408.
6. Haim M, Fledelius HC, Skarsholm . X-linked myopia in Danish family. *Acta Ophthalmol (Copenh)*. 1988;66(4):450–456.
7. Young TL, Deeb SS, Ronan SM, et al. X-linked high myopia associated with cone dysfunction. *Arch Ophthalmol*. 2004;122(6):897–908.
8. Michaelides M, Johnson S, Bradshaw K, et al. X-linked cone dysfunction syndrome with myopia and protanopia. *Ophthalmology*. 2005;112(8):1448–1454.
9. McClements M, Davies WI, Michaelides M, et al. Variations in opsin coding sequences cause X-linked cone dysfunction syndrome with myopia and dichromacy. *Invest Ophthalmol Vis Sci*. 2013;54(2):1361–1369.
10. Patterson EJ, Wilk M, Langlo CS, et al. Cone photoreceptor structure in patients with X-linked cone dysfunction and red-green color vision deficiency. *Invest Ophthalmol Vis Sci*. 2016;57(8):3853–3863.
11. Greenwald SH, Kuchenbecker JA, Rowlan JS, Neitz J, Neitz M. Role of a dual splicing and amino acid code in myopia, cone dysfunction and cone dystrophy associated with L/M opsin interchange mutations. *Transl Vis Sci Technol*. 2017;6(3):2.
12. Ueyama H, Muraki-Oda S, Yamade S, et al. Unique haplotype in exon 3 of cone opsin mRNA affects splicing of its precursor, leading to congenital color vision defect. *Biochem Biophys Res Commun*. 2012;424(1):152–157.
13. Mizrahi-Meissonnier L, Merin S, Banin E, Sharon D. Variable retinal phenotypes caused by mutations in the X-linked photopigment gene array. *Invest Ophthalmol Vis Sci*. 2010;51(8):3884–3892.
14. Neitz M, Patterson SS, Neitz J. Photopigment genes, cones, and color update: Disrupting the splicing code causes a diverse array of vision disorders. *Curr Opin Behav Sci*. 2019;30:60–66.
15. Li J, Gao B, Guan L, et al. Unique variants in OPN1LW cause both syndromic and nonsyndromic X-linked high myopia mapped to MYP1. *Invest Ophthalmol Vis Sci*. 2015;56(6):4150–4155.
16. Stingl K, Baumann B, De Angeli P, et al. Novel OPN1LW/OPN1MW exon 3 haplotype-associated splicing defect in patients with X-linked cone dysfunction. *Int J Mol Sci*. 2022;23(12):6868.
17. Guo X, Xiao X, Li S, et al. Nonsyndromic high myopia in a Chinese family mapped to MYP1: Linkage confirmation and phenotypic characterization. *Arch Ophthalmol*. 2010;128(11):1473–1479.
18. Wang Y, Xiao X, Li X, et al. Genetic and clinical landscape of ARR3-associated MYP26: The most common cause of

Mendelian early-onset high myopia with a unique inheritance [published online ahead of print September 30, 2022]. *Br J Ophthalmol*, doi:10.1136/bjo-2022-321511.

19. Wang Q, Wang P, Li S, et al. Mitochondrial DNA haplogroup distribution in Chaoshanese with and without myopia. *Mol Vis*. 2010;16:303–309.
20. Jiang D, Li J, Xiao X, et al. Detection of mutations in LRPAP1, CTSH, LEPREL1, ZNF644, SLC39A5, and SCO2 in 298 families with early-onset high myopia by exome sequencing. *Invest Ophthalmol Vis Sci*. 2014;56(1):339–345.
21. Li J, Jiang D, Xiao X, et al. Evaluation of 12 myopia-associated genes in Chinese patients with high myopia. *Invest Ophthalmol Vis Sci*. 2015;56(2):722–729.
22. Wang P, Li S, Sun W, et al. An ophthalmic targeted exome sequencing panel as a powerful tool to identify causative mutations in patients suspected of hereditary eye diseases. *Transl Vis Sci Technol*. 2019;8(2):21.
23. Neitz M, Neitz J. Intermixing the OPN1LW and OPN1MW genes disrupts the exonic splicing code causing an array of vision disorders. *Genes (Basel)*. 2021;12(8):1180.
24. Oda S, Ueyama H, Nishida Y, Tanabe S, Yamade S. Analysis of L-cone/M-cone visual pigment gene arrays in females by long-range PCR. *Vision Res*. 2003;43(5):489–495.
25. Ohno-Matsui K, Kawasaki R, Jonas JB, et al. International photographic classification and grading system for myopic maculopathy. *Am J Ophthalmol*. 2015;159(5):877–883. e877.
26. Patterson EJ, Kalitzeos A, Kasilian M, et al. Residual cone structure in patients with X-linked cone opsin mutations. *Invest Ophthalmol Vis Sci*. 2018;59(10):4238–4248.
27. Carroll J, Dubra A, Gardner JC, et al. The effect of cone opsin mutations on retinal structure and the integrity of the photoreceptor mosaic. *Invest Ophthalmol Vis Sci*. 2012;53(13):8006–8015.
28. Deeb SS, Lindsey DT, Hibiya Y, et al. Genotype-phenotype relationships in human red/green color-vision defects: Molecular and psychophysical studies. *Am J Hum Genet*. 1992;51(4):687–700.
29. Nathans J, Maumenee IH, Zrenner E, et al. Genetic heterogeneity among blue-cone monochromats. *Am J Hum Genet*. 1993;53(5):987–1000.
30. Nathans J, Davenport CM, Maumenee IH, et al. Molecular genetics of human blue cone monochromacy. *Science*. 1989;245(4920):831–838.
31. Patterson EJ, Kalitzeos A, Kane TM, et al. Foveal cone structure in patients with blue cone monochromacy. *Invest Ophthalmol Vis Sci*. 2022;63(11):23.
32. De Silva SR, Arno G, Robson AG, et al. The X-linked retinopathies: Physiological insights, pathogenic mechanisms, phenotypic features and novel therapies. *Prog Retin Eye Res*. 2021;82:100898.
33. Fahim AT, Sullivan LS, Bowne SJ, et al. X-chromosome inactivation is a biomarker of clinical severity in female carriers of RPGR-associated X-linked retinitis pigmentosa. *Ophthalmol Retina*. 2020;4(5):510–520.
34. Frederiksen AL, Duno M, Welinder LG. Blue cone monochromatism in a female due to skewed X-inactivation. *Ophthalmic Genet*. 2013;34(1-2):101–104.
35. Jacobson SG, Yagasaki K, Feuer WJ, Román AJ. Interocular asymmetry of visual function in heterozygotes of X-linked retinitis pigmentosa. *Exp Eye Res*. 1989;48(5):679–691.
36. Dacey DM. Circuitry for color coding in the primate retina. *Proc Natl Acad Sci USA*. 1996;93(2):582–588.
37. Jusuf PR, Martin PR, Grünert U. Random wiring in the midget pathway of primate retina. *J Neurosci*. 2006;26(15):3908–3917.
38. Kolb H, Marshak D. The midget pathways of the primate retina. *Doc Ophthalmol*. 2003;106(1):67–81.
39. Wiesel TN, Hubel DH. Spatial and chromatic interactions in the lateral geniculate body of the rhesus monkey. *J Neurophysiol*. 1966;29(6):1115–1156.
40. Crook JD, Manookin MB, Packer OS, Dacey DM. Horizontal cell feedback without cone type-selective inhibition mediates "red-green" color opponency in midget ganglion cells of the primate retina. *J Neurosci*. 2011;31(5):1762–1772.
41. Patterson SS, Neitz M, Neitz J. Reconciling color vision models with midget ganglion cell receptive fields. *Front Neurosci*. 2019;13:865.
42. Heeger DJ, Simoncelli EP, Movshon JA. Computational models of cortical visual processing. *Proc Natl Acad Sci USA*. 1996;93(2):623–627.
43. Neitz J, Neitz M. Evolution of the circuitry for conscious color vision in primates. *Eye (Lond)*. 2017;31(2):286–300.
44. Dacey DM, Lee BB, Stafford DK, Pokorny J, Smith VC. Horizontal cells of the primate retina: Cone specificity without spectral opponency. *Science*. 1996;271(5249):656–659.
45. Wool LE, Crook JD, Troy JB, et al. Nonselective wiring accounts for red-green opponency in midget ganglion cells of the primate retina. *J Neurosci*. 2018;38(6):1520–1540.
46. Zhang C, Kim YJ, Silverstein AR, et al. Circuit reorganization shapes the developing human foveal midget connectome toward single-cone resolution. *Neuron*. 2020;108(5):905–918.e903.
47. Neitz M, Wagner-Schuman M, Rowlan JS, Kuchenbecker JA, Neitz J. Insight from OPN1LW gene haplotypes into the cause and prevention of myopia. *Genes (Basel)*. 2022;13(6):942.
48. Rucker FJ, Kruger PB. Cone contributions to signals for accommodation and the relationship to refractive error. *Vision Res*. 2006;46(19):3079–3089.
49. Ingling CR, Jr., Martinez-Uriegas E. The relationship between spectral sensitivity and spatial sensitivity for the primate r-g X-channel. *Vision Res*. 1983;23(12):1495–1500.
50. Winderickx J, Battisti L, Motulsky AG, Deeb SS. Selective expression of human X chromosome-linked green opsin genes. *Proc Natl Acad Sci USA*. 1992;89(20):9710–9714.
51. Rappon J, Chung C, Young G, et al. Control of myopia using diffusion optics spectacle lenses: 12-month results of a randomised controlled, efficacy and safety study (CYPRESS) [published online ahead of print September 1, 2022]. *Br J Ophthalmol*, doi:10.1136/bjo-2021-321005.
52. Széll N, Fehér T, Maróti Z, et al. Myopia-26, the female-limited form of early-onset high myopia, occurring in a European family. *Orphanet J Rare Dis*. 2021;16(1):45.
53. Palczewski K. G protein-coupled receptor rhodopsin. *Annu Rev Biochem*. 2006;75:743–767.

Investigative Ophthalmology & Visual Science